JOURNAL OF APPLIED ELECTROCHEMISTRY 19 (1989) 500–504

The effect of metal and solution phase resistances on the current distribution in cylindrical electrochemical reactors

JOSÉ M. BISANG

Programa de Electroquímica Aplicada e Ingeniería Electroquímica (PRELINE), Facultad de Ingeniería Química, Universidad Nacional del Litoral, Santiago del Estero 2829, 3000 Santa Fe, Argentina

Received 16 August 1988; revised 12 January 1989

The mathematical modelling of cylindrical electrochemical reactors has been performed taking into account the resistance of the metal phase of the inner electrode and the resistance of the electrolyte. The model assumes that the external electrode is isopotential, the electrochemical reaction on the external electrode has a low polarization resistance ($di/d\eta \rightarrow \infty$) and at each axial position in the electrolyte the current is independent of the radial coordinate. The experimental and theoretical current density distributions are compared in order to determine the predictive suitability of the model and a good agreement is observed between them. Furthermore, a comparison is made between this model and a simpler earlier one and an important improvement in the prediction is observed.

Nomenclature

A	defined by Equation 27	($cm^2 A^{-1}$)
A_s	surface area per unit volume of electrode	(cm^{-1})
b	constant in the Tafel equation	(V^{-1})
B	constant defined by Equation 28	($\Omega cm^2 V^{-2}$)
C	constant defined by Equation 29	(Ω)
E_0	reversible electrode potential	(V)
i	current density	($A cm^{-2}$)
i_j	current density in j	($A cm^{-2}$)
i_0	exchange current density	($A cm^{-2}$)
I_j	current in the phase j	(A)
I	total current	(A)
L	electrode length	(cm)
r_j	radius of j	(cm)
r	radial coordinate	(cm)
U_0	reversible cell voltage	(V)
V	applied voltage to the reactor	(V)
x	axial coordinate	(cm)

Greek characters

$\bar{\delta}_r$	mean relative deviation	
η	overvoltage	(V)
ϱ	resistivity	(Ω cm)
ϕ	potential	(V)

Subscripts

e	external electrode
exp	experimental
i	internal electrode
m	metallic phase
s	solution phase
th	theoretical

1. Introduction

Methods to predict the distribution of current over electrode surfaces are of great interest in applied electrochemistry. Models are employed to design electrochemical reactors with the object of increasing their effectiveness and selectivity. Furthermore, they are used in the metal electrodeposition process in order to obtain more uniform coatings and in the design of systems for corrosion protection.

When the electrode is thin or the current is high it is very important to consider the resistance of the metal phase in the modelling of the reactors. In the literature, there are some mathematical analyses [1–4] evaluating such systems. Other authors [1, 5, 6] have also incorporated the resistance of the solution phase into their models, though the experimental verification of the model proposed has not been reported.

Current density distribution on a wire electrode was studied in previous work [7] carried out in this laboratory. The values measured experimentally were compared with those predicted by a model that considered only the resistance of the metal phase. All disagreements between model and experiments were attributed to the fact that the electrolyte was not considered by the model. This situation originated the present paper. Here the effect of the resistances of both phases – metal and solution – on the current distribution is analyzed.

2. Model considerations

The overall voltage balance for a cylindrical electrochemical reactor at the axial position x may be written

0021-891X/89 $03.00 + .12

as

$$V = U_0(x) + \Delta\phi_{m,i}(x) + \eta_i(x) + \Delta\phi_s(x) + \eta_e(x) + \Delta\phi_{m,e}(x) \quad (1)$$

where V is the voltage drop between the connection points of the anode and cathode, $U_0(x)$ is the reversible cell voltage, $\Delta\phi_{m,i}(x)$ is the ohmic drop in the metal phase of the inner electrode between its feeder point $x = 0$ and x, $\eta_i(x)$ is the overvoltage at the inner electrode, $\Delta\phi_s(x)$ is the ohmic drop in the solution phase in x, $\eta_e(x)$ and $\Delta\phi_{m,e}(x)$ are the overvoltage and the ohmic drop in the metal of the external electrode respectively.

In Equation 1 the six terms on the right hand side are a function of the axial position x but their sum is constant.

In the earlier model, reported in [7], the following terms were not considered to be a function of x:

- the reversible cell voltage,
- the ohmic drop in the electrolyte; this assumption is more realistic when its conductivity is high or when the current is small,
- the overvoltage at the external electrode; it is imperative that the electrochemical reaction has a high polarization curve slope ($di/d\eta \to \infty$),
- the ohmic drop in the metal phase of the external electrode; this electrode is easily accessed, therefore an electrical connection can be made in order to ensure isopotentiality.

With these assumptions, Equation 1 becomes:

$$\Delta\phi_{m,i}(x) + \eta_i(x) = \text{constant} \quad (2)$$

Since the constant in Equation 2 is independent of x, let us evaluate it at any position x, for example $x = 0$:

$$\Delta\phi_{m,i}(x) + \eta_i(x) = \eta_i(0) \quad (3)$$

When Equation 3 is satisfied, the model assumes that the cylindrical surface of the electrolyte in the neighborhood of the inner electrode is isopotential as postulated in the previous paper [7].

The second restriction above is partially suppressed in the new model and the other three conditions are preserved in it.

In this case, Equation 1 yields

$$\Delta\phi_{m,i}(x) + \eta_i(x) + \Delta\phi_s(x) = \text{constant} \quad (4)$$

The constant is again obtained evaluating the above equation at $x = 0$:

$$\Delta\phi_{m,i}(x) + \eta_i(x) + \Delta\phi_s(x) = \eta_i(0) + \Delta\phi_s(0) \quad (5)$$

In conclusion, the new model accepts that the cylindrical surface of the electrolyte in contact with the external electrode is now isopotential.

Additionally, at each axial position in the electrolyte the current will be considered independent of the radial coordinate, as is suggested by [5]; that is

$$I_s(x, r_i) = I_s(x, r) \quad (6)$$

Thus, each section of the external electrode takes the current from the inner electrode portion directly opposite to it.

3. Mathematical model

Considering that the inner electrode is a cylindrical rod of length, L, and radius, r_i, fed at its lower end ($x = 0$), the differential current balance is:

$$\frac{di_m(x)}{dx} = -A_s i[\eta(x)] \quad (7)$$

with

$$A_s = \frac{2}{r_i} \quad (8)$$

where $i[\eta(x)]$ is the current density on the inner electrode at the position x.

Integrating Equation 7 with $i_m(0) = i_i$ and $i_m(L) = 0$ gives

$$i_i = A_s \int_0^L i[\eta(x)]\, dx \quad (9)$$

and i_i is given by

$$i_i = \frac{I}{\pi r_i^2} \quad (10)$$

The overvoltage distribution along the inner electrode must be known in order to calculate I from Equations 9 and 10. By definition of overvoltage

$$\eta(x) = \phi_m(x) - \phi_s(r_i, x) - E_0 \quad (11)$$

Ohm's law for the metal phase may be written as

$$\frac{d\phi_m(x)}{dx} = -\varrho_m i_m(x) \quad (12)$$

Differentiating Equation 12 with respect to x, and introducing Equation 7 yields

$$\frac{d^2\phi_m(x)}{dx^2} = A_s \varrho_m i[\eta(x)] \quad (13)$$

Assuming Tafel kinetics

$$\frac{d^2\phi_m(x)}{dx^2} = A_s \varrho_m i_0 \exp[b\eta(x)] \quad (14)$$

Ohm's law for the solution phase is

$$\frac{d\phi_s(r, x)}{dr} = -\varrho_s i_s(r, x) \quad (15)$$

Taking account of Equation 6 gives

$$d\phi_s(r, x) = -\frac{\varrho_s I_s(x)}{2\pi L}\frac{dr}{r} \quad (16)$$

Integrating

$$\phi_s(r, x) - \phi_s(r_i, x) = -\frac{\varrho_s I_s(x)}{2\pi L}\ln\frac{r}{r_i} \quad (17)$$

Since

$$I_s(x) = 2\pi r_i L i[\eta(x)] \quad (18)$$

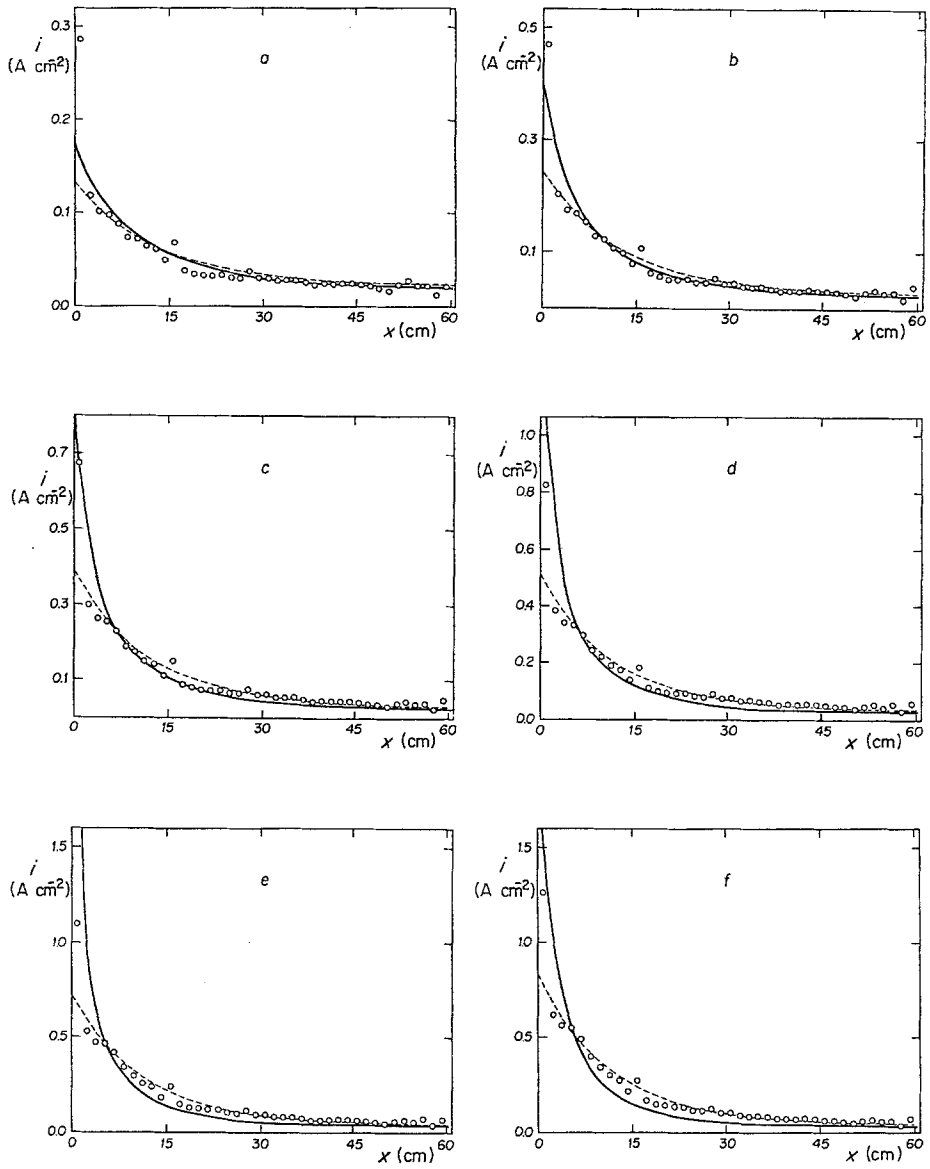

Fig. 1. Current distributions for hydrogen evolution. [NaOH] = 1 M; T = 30° C; (a) 0.174 A; (b) 0.271 A; (c) 0.392 A; (d) 0.486 A; (e) 0.639 A; (f) 0.727 A. (——) Former model; (– – –) new model; (○) experimental results.

Introducing Equation 18 into Equation 17 and solving for $r = r_e$ gives

$$\phi_s(r_e, x) - \phi_s(r_i, x) = -\varrho_s r_i i[\eta(x)] \ln \frac{r_e}{r_i} \quad (19)$$

Assuming that $\phi_s(r_e, x)$ is not a function of x, according to the isopotentiality condition of the electrolytic solution adjacent to the external electrode, Equation 19 becomes

$$\phi_s(r_i, x) - \phi_s(r_e) = \varrho_s r_i\, i[\eta(x)] \ln \frac{r_e}{r_i} \quad (20)$$

Taking derivatives twice with respect to x

$$\frac{d^2\phi_s(r_i, x)}{dx^2} = \varrho_s r_i \frac{d^2 i[\eta(x)]}{dx^2} \ln \frac{r_e}{r_i} \quad (21)$$

Considering the Tafel equation and differentiating it twice with respect to x

$$\frac{d^2 i[\eta(x)]}{dx^2} = i_0 b \exp [b\eta(x)] \left\{ b \left[\frac{d\eta(x)}{dx} \right]^2 + \frac{d^2\eta(x)}{dx^2} \right\} \quad (22)$$

Introducing Equations 14, 21 and 22 into the expression obtained from taking the second derivative with respect to x of Equation 11 yields

$$\frac{d^2\eta(x)}{dx^2} = \varrho_m A_s i_0 \exp [b\eta(x)] - \varrho_s r_i \ln \frac{r_e}{r_i} i_0 b \times \exp [b\eta(x)] \left\{ b \left[\frac{d\eta(x)}{dx} \right]^2 + \frac{d^2\eta(x)}{dx^2} \right\} \quad (23)$$

Rearranging Equation 23 gives

$$A[\eta(x)] \frac{d^2\eta(x)}{dx^2} + B \left[\frac{d\eta(x)}{dx} \right]^2 - C = 0 \quad (24)$$

where

$$A[\eta(x)] = \frac{\exp [-b\eta(x)]}{i_0} + \varrho_s r_i \ln \frac{r_e}{r_i} b \quad (25)$$

$$B = \varrho_s r_i \ln \frac{r_e}{r_i} b^2 \quad (26)$$

$$C = \varrho_m A_s \quad (27)$$

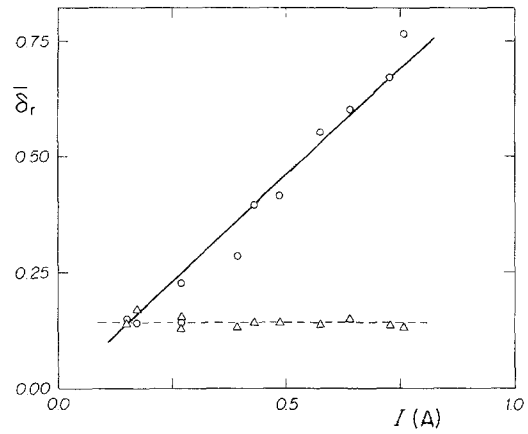

Fig. 2. $\bar{\delta}_r$ as a function of the total current. [NaOH] = 1 M; T = 30° C. (——) Former model; (- - -) new model.

with the following boundary conditions:

$$x = 0 \qquad \eta(x) = \eta(0) \tag{28}$$

$$x = 0 \qquad \left.\frac{d\eta(x)}{dx}\right|_{x=0} = \frac{-\varrho_m i_i}{1 + \varrho_s r_i \ln \frac{r_e}{r_i} i_0 b \exp[b\eta(0)]} \tag{29}$$

The solution of this system was obtained numerically by means of a combination of a *regula falsi* method with a finite difference method.

4. Experimental details and results

The distributions of current densities were determined using the segmented counter electrode method. The working electrode was a Pt wire, of 0.2 mm diameter and 600 mm long, centrally positioned. The counter electrode was made of 40 304 stainless steel rings, 41.35 mm internal diameter, 1.5 mm thick and 14 mm high, each ring being separated by an O-ring approximately 1 mm thick. The attached resistance at each segment was 0.09 Ω. A detailed description of the equipment employed, method of operation, test reaction and reagents has been given previously in [7].

Figure 1 shows some typical current density curves as a function of position for different total currents. Hydrogen evolution from 1 M NaOH solution at 30° C was used as the test reaction.

Figure 2 summarizes these results; the mean relative deviation, $\bar{\delta}_r$ with regard to each model, was

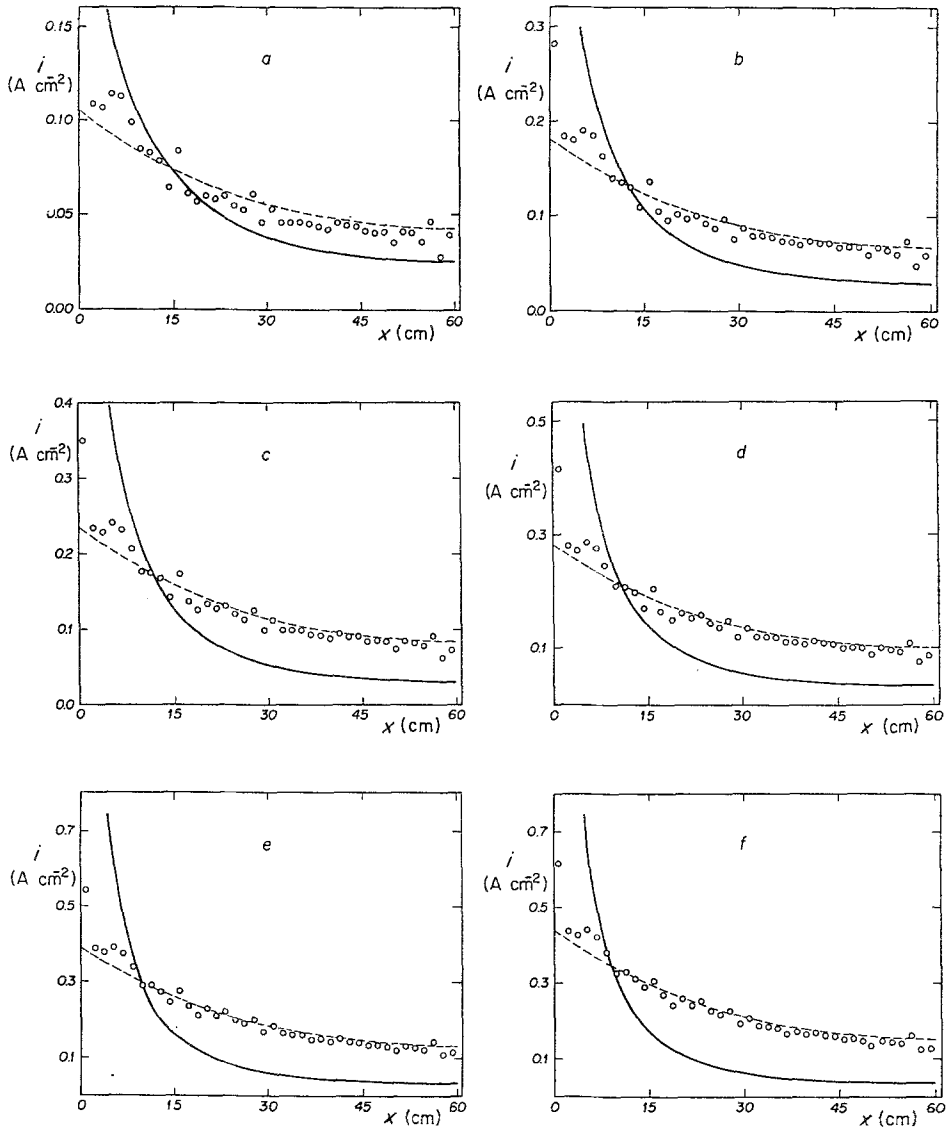

Fig. 3. Current distributions for hydrogen evolution. [NaOH] = 0.1 M; T = 30° C; (a) 0.232 A; (b) 0.384 A; (c) 0.490 A; (d) 0.582 A; (e) 0.794 A; (f) 0.896 A. (——) Former model; (- - -) new model; (○) experimental results.

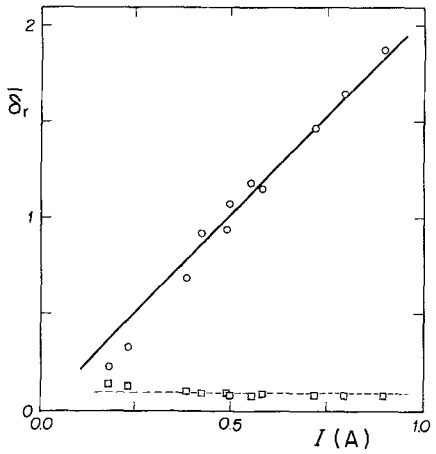

Fig. 4. $\bar{\delta}_r$ as a function of the total current. [NaOH] = 0.1 M; T = 30° C. (——) Former model; (– – –) new model.

represented as a function of the total current. The mean relative deviation was computed using the following expression:

$$\bar{\delta}_r = \frac{1}{40} \sum_{j=1}^{40} \frac{|i_{exp}(x_j) - i_{th}(x_j)|}{i_{th}(x_j)} \qquad (30)$$

Figure 3 shows some typical curves of the current density versus position for hydrogen evolution from 0.1 M NaOH solution at 30° C. The corresponding mean relative deviations are given in Figure 4.

5. Discussion and conclusions

When analyzing the four figures, it is observed that both models have the same predictive capability if the current is low, although when the current increases the new model gives the best prediction which is practically independent of the total current. The average values of the mean relative deviation are 14.23% for the concentrated solution and 9.46% for the dilute solution.

The experimental results lie between the two theoretical curves, but they approach the new model when the current is higher. This is more evident in the case of the dilute solution (Fig. 3).

As seen in the figures, the current densities predicted by the model that only includes the resistance of the metal phase are higher than the experimental results for low values of x. The opposite is observed in the region far from the feeding point. This behavior occurs because the resistance of the solution phase, which will tend to make the current distribution more uniform [7], has not been included in the model. The high current densities calculated in the portion of the inner electrode near the feeding point leads to a computed ohmic drop for the metal phase in this region that is higher than the real ohmic drop, therefore producing low values in the calculated η and i at high x, according to Equation 3.

The current densities predicted by the model that includes the resistance of the electrolyte are lower than the experimental values in the region near the feeding point, and larger than the experimental values far from it. This occurs because the present model accepts the validity of Equation 6 when actually the real system should show a current distribution in the solution phase, I_s, that depends on the axial as well as on the radial coordinate. Therefore, for low values of x, the total current in the electrolyte should be larger near the inner electrode than anywhere else, that is

$$I_s(x, r_i) > I_s(x, r) \qquad (31)$$

Consequently, in the region of low values of x, the model predicts higher ohmic drops in the solution phase than those existing in the actual system. This effect produces, according to Equation 4, calculated overvoltages and current densities smaller than those obtained experimentally. Furthermore, the low predicted current density in the neighborhood of the feeding point produces an ohmic drop in the metal phase that is small than the real ohmic drop, thus leading to high theoretical i values at high x.

Finally, from this work it is concluded that taking into account the resistances of both phases – solution and metal – the predictive capability of the model is increased, thereby allowing the use of this mathematical treatment to design such reactors even for high currents or dilute solutions.

Acknowledgement

The author would like to thank Stiftung Volkswagenwerk and Deutscher Akademischer Austauschdienst (DAAD) of the Federal Republic of Germany for donating scientific equipment.

References

[1] C. W. Tobias and R. Wijsman, *J. Electrochem. Soc.* **100** (1953) 459.
[2] B. E. Conway, E. Gileadi and H. G. Oswin, *Can. J. Chem.* **41** (1963) 2447.
[3] S. K. Ranjarajan, M. J. Dignam and B. E. Conway, *Can. J. Chem.* **45** (1967) 422.
[4] J. Wojtowicz, L. Laliberté and B. E. Conway, *Electrochim. Acta* **13** (1968) 361.
[5] R. Alkire and R. Varjian, *J. Electrochem. Soc.* **121** (1974) 622.
[6] K. Hertwig and J. Breme, *Chem. Techn. (Leipzig)* **32** (1980) 294.
[7] J. M. Bisang and G. Kreysa, *J. Appl. Electrochem.* **18** (1988) 422.